Evaluation of Drivers' Interaction Ability at Social Scenarios: A Process-Based Framework

Preprint *in* SSRN Electronic Journal · March 2023

DOI: 10.2139/ssrn.4370155

4 authors:

Jiaqi Liu
Tongji University
8 PUBLICATIONS **0** CITATIONS
SEE PROFILE

Peng Hang
Tongji University
79 PUBLICATIONS **1,198** CITATIONS
SEE PROFILE

Jian Sun
Tongji University
229 PUBLICATIONS **4,445** CITATIONS
SEE PROFILE

Xiangwang Hu
Soochow University (PRC)
5 PUBLICATIONS **142** CITATIONS
SEE PROFILE

Evaluation of Drivers' Interaction Ability at Social Scenarios: A Process-Based Framework

Jiaqi Liu, Peng Hang, Xiangwang Hu* and Jian Sun

Department of Traffic Engineering & Key Laboratory of Road and Traffic Engineering, Ministry of Education, Tongji University, China

ARTICLE INFO

Keywords:
Interaction Ability Evaluation
Game Theory
Driving Risk Perception
Behavior Similarity Measures

ABSTRACT

The evaluation of the drivers' interaction abilities is quite important for understanding human drivers' behaviors and improving autonomous vehicles' interaction abilities. Taking the unprotected left turn maneuver as an instance, existing turn-left interaction ability evaluation indicators are designed based on the interaction result analysis, and there is a lack of process-oriented capability evaluation methods. In this paper, a three-stage interaction ability evaluation framework is proposed, including Interaction Risk Perception, Interaction Process Modeling, and Interaction Ability Scoring, which is designed to interpret and assess the social behaviors of drivers during the interaction process. The evaluation framework defines different types of excellent action benchmarks based on the game theoretic approach, which is considered as the ability evaluation standard. Then an improved evaluation index based on morphological similarity distance is proposed, which is used to calculate the action gaps between the real-world driver and the rational person, so the driver's interaction ability is scored. By adjusting the driving preference of the benchmark, the safety and efficiency preference, and the interactive sociality of drivers during the interaction are dug and evaluated. We compare the interaction ability of Chinese and US drivers and find that there are significant differences between the two groups: Chinese drivers have higher radical and competitive behaviors, while US drivers are more conservative and cooperative.

1. Introduction

In the future human-machine mixed driving environment, autonomous vehicles (AVs) need to understand the social intentions of other drivers and drive in a way that meets human expectations. Understanding and evaluating the interaction behaviors of drivers are the key for AV to predict the future states of human drivers and generate recognizable social driving behaviors(Parkin, Clark, Clayton, Ricci and Parkhurst (2016); Nilsson, Thill and Ziemke (2015)). But understanding human-driver interactions on the road is very difficult for AVs because human beings do not simply obey traffic rules like machines. To achieve safety and efficiency gains, they obey implicit social norms and rules (Wang, Wang, Zhang, Liu and Sun (2022a)). Therefore, simple quantitative indicators and rigid traffic rules cannot be used to evaluate their behaviors.

In recent years, Time to Collision (TTC)(Fiorentino and Parseghian (1997)) and Post Encroachment Time (PET)(Qi, Wang, Shen and Wu (2020)) are always used to assess and analyze the interaction between vehicles. These indicators can reflect consequential information such as the safety of interaction events after the interaction is completed. Still, the interaction process and the ability of both parties have not been assessed(Markkula, Madigan, Nathanael, Portouli, Lee, Dietrich, Billington, Schieben and Merat (2020)). Data-driven methods such as deep neural networks have shown exemplary performance in quantifying interactions. However, the mechanisms of these approaches are poorly interpretable, and difficult to provide reliable evaluation criteria(Wang et al. (2022a)). The model-based method has a clearer structure and better interpretability, in which game theory is widely used to analyze the interaction process and model the interaction(Li, Liu and Xiao (2022)). The game model can accurately capture the dynamic interactions from drivers and provide a basis for describing the spatiotemporal characteristics of driving behaviors.

To this end, this paper proposes a process-oriented framework to evaluate the driving ability of drivers in dynamic and interactive scenarios, which contains three stages: Risk Perception Modeling, Interaction Process Modeling, and

*Corresponding author

liujiaqi13@tongji.edu.cn (J. Liu); hangpeng@tongji.edu.cn (P. Hang); huxiangwang@tongji.edu.cn (X. Hu); sunjian@tongji.edu.cn (J. Sun)

ORCID(s): 0000-0002-6171-6155 (J. Liu)

Interaction Ability Scoring. This framework is designed to assess the social interaction behaviors in road traffic, especially in complex interaction scenarios.

In the framework, we proposed the rational person model, which applies the non-cooperative and cooperative games respectively to model the action responses of different drivers in the interaction process. Rational persons with different styles can be derived by adjusting the weight of the payoff function of the game. After quantifying the driver's perceived risk, the rational person model outputs different driving behavior benchmarks by using the rational person model with other social preferences. And then, a driver's social abilities (e.g. safety, efficiency, and sociality) will be evaluated by calculating the gap between his action and the excellent action benchmark. Furthermore, we apply our framework to the unprotected left-turn scenarios in China and the United States, and the difference in driving ability between the two countries' drivers is compared.

Compared with the existing evaluation indicators, this framework is process-based. It could assess different social driving characteristics of road users and analyze what happened during the interaction, which may be beneficial for AVs to identify the social cues of other road participants.

The contributions of this paper are as follows:

- A three-stage ability evaluation framework for challenging and interactive scenes is proposed, including Risk Perception Modeling, Interaction Process Modeling, and Interaction Ability Scoring. Compared with the existing evaluation indicators, this framework is process-based and can analyze drivers' performance and show what happened during the interaction;
- In the part of Interaction Process Modeling, a rational person model based on the game theoretic approach is established. The rational person will confront the interaction conditions as same as the real-world driver and output the decision-making results. The driving characteristics during the interaction can be detected and evaluated by digging into differences between the real-world driver and the ration person;
- In the framework, a comprehensive risk perception model is established, which combines the instantaneous state risk and future state risk in the traffic scenario. The Extended Kalman Filter (EKF) is used to estimate the feature vehicle motion states. And a novel improved morphological similarity evaluation index is proposed to measure the gap between reality and rationality. Furthermore, the unprotected left-turn scenario is selected as a typical testing scenario, and the social abilities of Chinese and US drivers have been assessed by using different datasets.

The rest of the paper is organized as follows: Section 2 summarizes the recent related works. The overview of the proposed evaluation framework is presented in section 3. In section 4, detailed information about the framework is introduced. In section 5, different datasets are used for evaluation experiments and the results are analyzed. Finally, this paper is concluded in section 6.

2. Literature Review

2.1. Driving Interaction Behavior Modeling and Assessment

Constructing a model that can accurately describe the interactive process of drivers is the basis of evaluating the interaction behavior. In essence, human driving behavior is a game-theoretic problem(Wang, Wang, Zhang, Liu and Sun (2022b)). Human drivers are influenced by others to make decisions and then affect others, which forms a closed-loop dynamic game. The developed models using game theory to simulate driver-driver interaction have been widely used to evaluate and predict the driving behaviors of human drivers and design the interaction strategies between autonomous driving and human-driver vehicles(Tian, Li, Kolmanovsky, Yildiz and Girard (2020); Li, Liu and Xiao (2021); Cai, Hang and Lv (2021)). The performance of these models is usually evaluated by assessing the AVs' predicted trajectories.

However, the ability of human drivers is usually evaluated by driving simulation experiments and more detailed data analysis(Norris, Matthews and Riad (2000); Crizzle, Classen, Bedard, Lanford and Winter (2012)). This is because the information just from trajectories is limited, which can not fully reflect the drivers' intentions and actions in the interaction process and the driving ability behind these. Moreover, it is also unrealistic for a large number of real-time interaction evaluation needs in the future to meet by conducting driving simulation experiments. Therefore, how to make better use of output information of the game model to better evaluate drivers is a problem worth exploring.

2.2. Risk Quantification and Evaluation

Plenty of methods have been used to model the risk of vehicle motions. The existing risk assessment methods mainly include risk quantification index, collision prediction, risk field modeling, and so on.

It is a common and effective way to quantify the risk of moving objects by using indexes based on time or distance. The quantifying indexes based on time include TTC, time headway (THW), time margin (TM) and PET (Zhao, Li, Xie, Bi, Lu and Li (2018); Xiong, Wang, Cai, Chen, Farah and Hagenzieker (2019); Liu, He and Zhu (2019); Qi et al. (2020)), and stopping distance, safety margin are commonly used as the quantifying indexes based on distance(Doi and A (1994); Shalev-Shwartz, Shammah and Shashua (2017, 2018)).

By predicting feature trajectories of the interactive objects, evaluation methods based on collision prediction can calculate the risk of the collision. The motion trajectories of vehicles are normally predicted by deep learning models or linear differential equations, and the intersection point between two trajectories can be computed efficiently (Hillenbrand, Spieker and Kroschel (2006); Miller and Huang (2002)).

Meanwhile, the filed theory is also a common way to assess movement risks(Li, Gan, Ji, Qu and Ran (2020)). The concept of artificial potential field (APF) based on field theory was first proposed by Khatib(Kathib (1986)). The APF is also used as the basis to calculate the total potential of the traffic environment(Wang, Wang, Wan, Chu and Lu (2019)).

Although the methods mentioned above are widely studied and applied, how to better carry out a risk assessment in a complex interactive intersection is still a very challenging problem.

2.3. Performance Scoring and Similarity Evaluation.

The interactive ability evaluation problem of drivers can be converted to the motion similarity measurement problem between real-world drivers and excellent drivers. There are three kinds of dimensions for motion similarity measurement: (1) Measuring spatial similarity, which focuses on geometric trajectory and ignores time dimension, including Euclidean Distance (Little and Gu (2001)); (2) Measuring temporal similarity, which analyzes the temporal characteristic of sequence data, such as cosine similarity (Tetsuya, Nakamura, Keishi, Taki, Hiroki, Nomiya, Kazuhiro, Seki, Kuniaki and Uehara (2013)), etc.; (3) Measuring spatial-temporal similarity, which considers both spatial and temporal dimensions of motion data, and common method includes dynamic time warping (DTW) (Keogh (2002)).

Nevertheless, a single index of spatial similarity and temporal similarity evaluation mentioned above fails to capture many important features from the action sequences of drivers, and the spatial-temporal similarity evaluation index such as DTW can't normalize the difference between sequences into a finite interval, which is not able to satisfy the need for action evaluation and scoring.

3. Overview of the Evaluation Framework

In this section, the evaluation framework is outlined and an unprotected left-turn scenario is introduced, which is regarded as a typical instance to illustrate our framework in detail.

As exhibited in Figure 1, the interactive ability evaluation framework we proposed consists of three parts: Risk Perception Modeling, Interactive Process Modeling, and Interactive Ability Scoring. When interacting with other traffic participants, drivers usually assess the states of themselves, their potential interaction objects, and the environment to ensure safety before making a decision. So the proposed evaluation framework first evaluates interaction risk by motion state estimation and motion risk quantification. Then we propose the rational person model based on the game theory, which takes the results of risk evaluation as input. The rational person model is not always realistic because it assumes that all players during the interaction are perfectly rational, which is not the case. The drivers in the real world will perform worse than perfectly rational players due to various irrational behaviors. Therefore, the solutions of the game model are defined as the excellent sequence of rational human actions, which is used as the benchmark to evaluate the actual interaction ability of drivers. Finally, a novel assessment index is designed in the Interactive Ability Scoring part, which takes the actions of the real-world drivers and rational drivers from the game model as input, and the ability and social characteristics of drivers are scored. A detailed description of the three functional modules is presented as follows.

- **Risk Perception Modeling**: By motion state estimation with instantaneous states and EKF, the future states of drivers are obtained. And the risk between drivers is calculated by risk field theory. The proposed risk model combines the instantaneous state risk and future state risk, which quantifies the risk of the static and dynamic objects in the traffic environment;

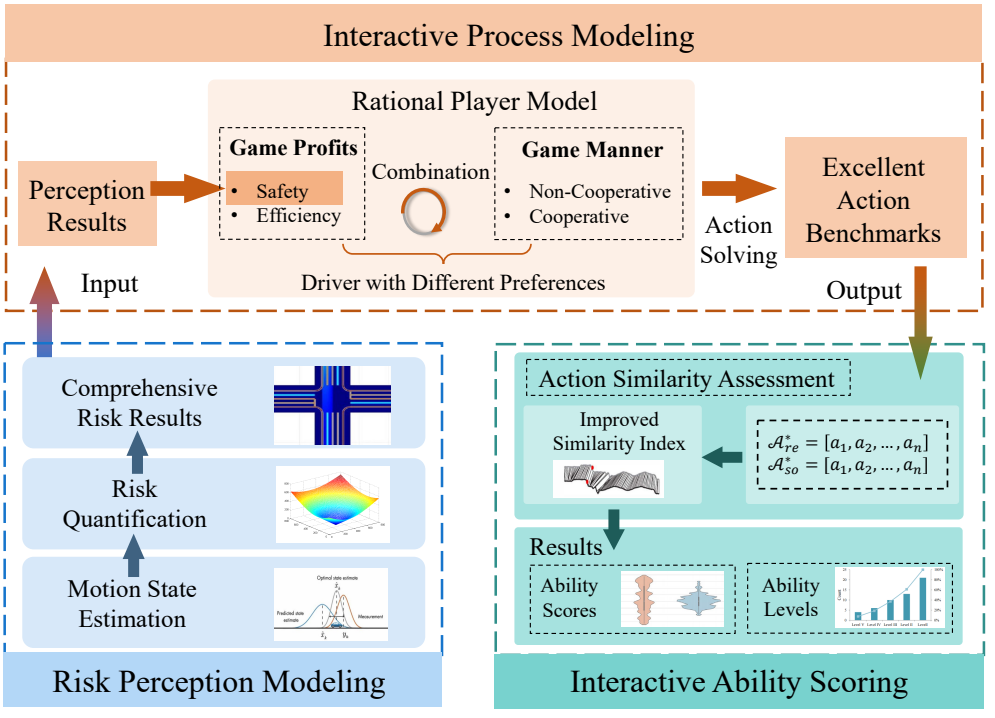

Figure 1: The framework of the interaction ability evaluation.

- **Interactive Process Modeling**: The rational person model is constructed first, taking the results of risk perception as game safety benefits. The sum of safety benefits and efficiency benefits is used to construct the player's total game benefit function, and the rational player will make decisions and take actions based on the maximum game payoff at each time step. By adjusting the game model, the rational players with different preferences are set up;
- **Interactive Ability Scoring**: An improved morphological similarity evaluation index is proposed. The scores and rankings of drivers who participated in the experiments are obtained by measuring the action gaps between actions from real-world drivers and rational actions from game models with different preferences.

There are many social interaction scenarios and behaviors when drivers move forward on the road, and making an unprotected left turn at an intersection is one of the most complex and challenging scenarios(Rahmati, Hosseini and Talebpour (2021)). We use this scenario as a typical case to model and illustrate our evaluation framework in the following parts.

When a driver makes an unprotected left turn at an intersection, there will be potential conflicts with the straight vehicle in the opposite lane, and interaction will occur in the process of determining the passing sequence. In our work, for simplicity, we mainly show the interaction between one unprotected left-turn driver and one straight driver at an intersection, as displayed in Figure2, and the framework will be expanded to multi-driver scenarios in the future.

4. Design of The Evaluation Framework

In this section, the evaluation framework is introduced in detail, including Risk Perception Modeling, Interactive Process Modeling, and Interactive Ability Scoring.

4.1. Risk Perception Modeling

When turning left at an intersection, a driver needs to find a suitable turn-left gap to pass under safe constraints. In order to ensure driving safety, the driver will not only consider the risk of the traffic environment at the moment but also predict the feature risk of reaching the conflict point based on the motion state of the interaction object. Therefore,

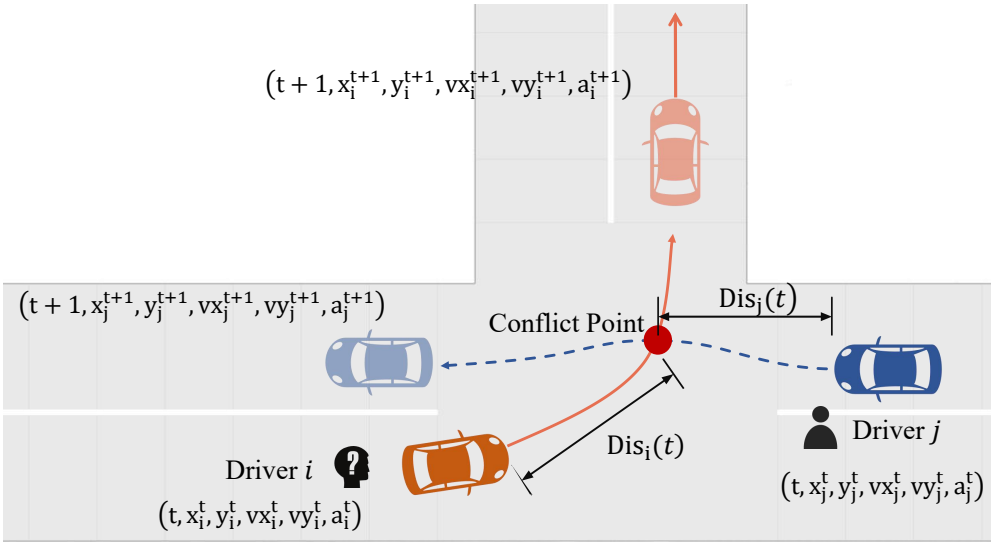

Figure 2: The interaction between one turn-left vehicle and one straight vehicle at the unprotected turning intersection.

the comprehensive motion risk is proposed, which is defined as the sum of the instantaneous state risk and the future state risk. And the risk field is used to quantify the perceived risk during the whole interaction process(Tan, Lu and Liu (2021)).

4.1.1. Instantaneous State Risk

According to the risk field theory, the physical objects in the traffic environment are divided into dynamic objects and static objects, and the modeling calculation is carried out respectively(Wang, Wu, Zheng, Ni and Li (2016)). Dynamic objects include entities whose moving speeds are greater than 0 or may be greater than 0 (motor vehicles, non-motor vehicles, pedestrians, etc.), and static objects include static obstacles, traffic lines, etc. To quantify the instantaneous state risk of the driver, the longitudinal driving risk model in (Tan et al. (2021)) is referenced.

In the Cartesian coordinate system, to quantify the risk of driver d, all the moving objects (vehicles) i ($i \in \{1, 2, \dots n\}$) around driver d are considered. Let $[x(k), y(k)]$ denote the Cartesian coordinates of driver d at k^{th} time interval. And the risk factor in the x-axis direction is defined as:

$$\delta_i(x(k)) = \frac{\beta_x \max(x(k) - (x_i + \frac{L_i}{2}, 0))}{\alpha_x v_{i,x}(t) + 1} \tag{1}$$

where β_x and α_x are the attenuation coefficients of the attenuation function of vehicle i on distance and speed, respectively, which represent the effect of the speed and relative distance of moving object on the longitudinal risk, $v_{i,x}$ is the velocity component of the vehicle i in the x-axis direction at k^{th} interval, x_i and L_i are the x coordinate of the vehicle i and the length of the vehicle i, respectively.

The risk function in the x direction is defined as:

$$\mathbf{R}_{i,longi}(x(k)) = \frac{1}{\delta_i(x(k)) + 1} \tag{2}$$

Also for the y direction, the decay factor and hazard function are:

$$\delta_i(y(k)) = \frac{\beta_y \max(y(k) - (y_i + \frac{W_i}{2}), 0)}{\alpha_y v_{i,y}(t) + 1} \tag{3}$$

$$\mathbf{R}_{i,lateral}(y(k)) = \frac{1}{\delta_i(y(k)) + 1} \tag{4}$$

where W_i is the width of the vehicle i.

Considering the risk attenuation in the x and y directions comprehensively, we have:

$$\delta_i(x(k), y(k)) = \sqrt{\delta_i^2(x(k)) + \delta_i^2(y(k))} \tag{5}$$

The risk function is defined as

$$\mathbf{R}_i(x(k), y(k)) = \frac{1}{\delta_i(x(k), y(k)) + 1} \tag{6}$$

For all static objects $j(j \in \{1, 2, ..., m\})$, it is equivalent to a moving object with a speed of 0, and the corresponding risk function is derived by

$$\mathbf{R}_{lane,j} = a_j \frac{1}{\delta_j(x, y) + 1} \tag{7}$$

where a_j denotes the maximum risk of the j_{th} road line.

The risk values of all dynamic entities and static entities are superimposed to obtain the global instantaneous state risk field.

$$\mathbf{R}_{now}(x(k), y(k)) = \sum_{i=1}^{n} \mathbf{R}_{veh,i}(x(k), y(k)) + \sum_{j=1}^{m} \mathbf{R}_{lane,j}(x(k), y(k)) \tag{8}$$

4.1.2. Future State Risk

The EKF model is used to estimate the movement of the interactive vehicle for the next observation interval, which is a nonlinear version of the Kalman filter. EKF estimates a vehicle's location with the state equation and observation equation first and then updates the vehicle's location.

Let $\mathbf{X}(k) = [x(k)\ y(k)\ v(k)\ \theta(k)]^T$, the estimated vehicle's state at $k + 1^{th}$ interval is described as follows.

$$\mathbf{X}_{k+1} = g(\mathbf{X}(k), u(k)) \tag{9}$$

where $\mathbf{X}_k$ represents the vehicle's state vector at k^{th} interval, $[x(k)\ y(k)]$ denotes the Cartesian coordinates at k^{th} interval, $v(k)$, $\theta(k)$ and $u(k)$ represent its speed, its heading angle and its actions at k^{th} interval, respectively.

For motion prediction, the following unicycle model is used.

$$\begin{bmatrix} x(k+1) \\ y(k+1) \\ v(k+1) \\ \theta(k+1) \end{bmatrix} = g(\mathbf{X}(k), u(k)) = \begin{bmatrix} x(k) + v(k)\cos(\theta(k))\Delta t \\ y(k) + v(k)\sin(\theta(k))\Delta t \\ v(k) + a(k)\Delta t \\ \theta(k) + \omega(k)\Delta t \end{bmatrix} \tag{10}$$

where $a(k)$ and $\omega(k)$ represent the acceleration and yaw rate of the vehicle.

The EKF uses linear transformations to approximate nonlinear relationships. Specifically, the EKF linearizes the motion by taking partial derivatives of the process equations and using first-order Taylor expansions.

Firstly, the Jacobian matrix of $X(k)$ is computed.

$$\mathbf{J}_A(k) = \begin{bmatrix} \frac{\partial x(k)}{\partial x} & \frac{\partial x(k)}{\partial y} & \frac{\partial x(k)}{\partial v} & \frac{\partial x(k)}{\partial \theta} \\ \frac{\partial y(k)}{\partial x} & \frac{\partial y(k)}{\partial y} & \frac{\partial y(k)}{\partial v} & \frac{\partial y(k)}{\partial \theta} \\ \frac{\partial v(k)}{\partial x} & \frac{\partial v(k)}{\partial y} & \frac{\partial v(k)}{\partial v} & \frac{\partial v(k)}{\partial \theta} \\ \frac{\partial \theta(k)}{\partial x} & \frac{\partial \theta(k)}{\partial y} & \frac{\partial \theta(k)}{\partial v} & \frac{\partial \theta(k)}{\partial \theta} \end{bmatrix} \tag{11}$$

Then, the predicted state information of the vehicle is updated as follows Schuhmann, Hofmann and Werner (2011); Schubert, Adam, Obst, Mattern, Leonhardt and Wanielik (2011).

$$\hat{\mathbf{X}}(k+1|k) = g(\mathbf{X}(k), u(k)) \tag{12}$$

$$\mathbf{P}(k+1|k) = \mathbf{J}_A(k)\mathbf{P}(k)\mathbf{J}_A(k)^T + \mathbf{Q}_k \tag{13}$$

where $\hat{\mathbf{X}}(k+1|k)$ denotes the estimated value at $k+1^{th}$ interval with previous k states, $\mathbf{Q}(k)$ is the covariance matrix of noise in state k, $\mathbf{P}(k+1|k)$ denotes the predicted covariance matrix of the state of the vehicles.

In our framework, the real position, velocity, and acceleration information of vehicles can be obtained from data and exchanged. The observation vector $\mathbf{V}(k)$ can be written as

$$\mathbf{V}(k) = \mathbf{H}(k)X(k) + \mathbf{Z}(k) \tag{14}$$

where $\mathbf{H}(k) = \begin{bmatrix} 1 & 0 & 0 & 0 \\ 0 & 1 & 0 & 0 \end{bmatrix}$, $\mathbf{Z}(k)$ is the noise vector, which satisfies the normal distribution:$\mathbf{V}(k) \sim N(0, \mathbf{R}(k))$. **R(k)** is the covariance matrix of noise at k^{th} interval.

Besides, the Kalman gain is updated by

$$\mathbf{K}(k+1) = \mathbf{P}(k+1|k)H^T[\mathbf{H}(k)\mathbf{P}(k|k-1)H^T(k) + \mathbf{R}(k)]^{-1} \tag{15}$$

The optimal estimation $\hat{\mathbf{X}}(k+1)$ of current state k+1 is

$$\hat{\mathbf{X}}(k+1) = \hat{\mathbf{X}}(k+1|k) + \mathbf{K}(k+1)[Z(k+1) - H(k+1)\hat{\mathbf{X}}(k+1|k)] \tag{16}$$

The error equation is derived by

$$\mathbf{P}(k+1) = \mathbf{P}(k+1|k) - \mathbf{K}(k+1)\mathbf{H}(k+1)\mathbf{P}(k+1|k) \tag{17}$$

where $\mathbf{P}(k+1|k)$ is the vehicle's predicted covariance matrix of state k.

Finally, the future state risk field is expressed as

$$\mathbf{R}_{fe}(x(k), y(k)) = \sum_{i=1}^{n} \mathbf{R}_{veh,i}(\hat{x}(k+1), \hat{y}(k+1)) + \sum_{j=1}^{m} \mathbf{R}_{lane,j}(x(k), y(k)) \tag{18}$$

4.1.3. Comprehensive Risk Perception

The instantaneous state risk and future state risk are superimposed to obtain the quantification results of comprehensive risk perception from the global perspective.

$$\mathbf{R}_{all} = \mathbf{R}_{now}(x(k), y(k)) + \mathbf{R}_{fe}(x(k), y(k)) \tag{19}$$

4.2. Interactive Process Modeling

The interaction between two drivers is a dynamic and complex behavioral process. During this process, drivers adjust their behaviors dynamically according to the actions of other drivers. Game theory can effectively describe this process, which assumes that all participants take actions under completely rational conditions, and an equilibrium solution can be obtained by solving the model. However, the drivers in the real world are not completely rational, and their game performance will be worse than completely rational players. Therefore, the game model solutions are defined as excellent interactive actions of the rational person, considered as the criterion for evaluating the interaction ability of the driver from the real world.

According to the game theory(Barron (2013)), there are at least three elements in the model: players, strategies, and profits. Assuming that there are n drivers interacting at an intersection, and the set of game players is $\mathcal{C} = \{C_L, C_S\}$, where C_L is the set of the left-turn drivers, C_S is the set of the straight drivers. The driver's strategy set is $S = \{s_1, s_2, s_3\}$, where s_1, s_2 and s_3 represent acceleration , uniform speed and deceleration, respectively. The position and speed states of driver i at k^{th} time interval are determined by his historical acceleration set $\mathcal{A}_i^{k-1}$, where $\mathcal{A}_i^{k-1} = (a_i^0, a_i^1, \ldots, a_i^{k-1})(1 \le k \le T-1)$, and the total benefits of driver i u_i^k during game process is also determined by the same set $\mathcal{A}_i^{k-1}$, remember to $u_i^k = \Phi(a_i^0, a_i^1, \ldots, a_i^{k-1}) = \Phi(\mathcal{A}_{k-1}^i)$.

Let $v_i(k-1)$ denote velocity of player i at $k-1^{th}$ time interval. When taking action at k^{th} time interval, the speed during interval $[k-1, k)$ is updated as

$$v_i(k) = v_i(k-1) + a_i(k)\Delta t \tag{20}$$

where $a_i(k)$ represents corresponding acceleration or deceleration action player i takes from strategies at k^{th} time interval.

Then the travel distance and estimated travel time of player i are calculated by the following function.

$$s_i(k) = s_i(k-1) + v_i(k)\Delta t \tag{21}$$

$$t_i = \frac{L_i - s_i(k)}{v_i(k) + \epsilon} \tag{22}$$

where $s_i(k)$ denotes the travel distance of player i at k^{th} time interval, $s_i(0) = 0$, L_i is the distance to the conflict point of player i at the intersection, and ϵ is a tiny positive constant which can ensure the function to be well-defined.

The type of game model and setting of the player benefit function will significantly affect the results of the model. From the perspective of an individual driver, safety, and efficiency are the two most important factors affecting the driver's decision-making, so the safety and efficiency benefits are considered as the payoff for players. To evaluate the performance of drivers in various aspects, three kinds of rational persons with different driving preferences are defined by adjusting players' benefit functions.

To evaluate driving safety and travel efficiency, three preferred rational persons, i.e., safety-first, efficiency-first, and comprehensive-type are defined.

Safety-first Rational Person: The driver who only considers safety risk when making decisions. The game benefit function of the player is written as

$$us_i^k(\alpha_i) = 1 - R_i(k) \tag{23}$$

Efficiency-first Rational Person: The driver who only takes the prevailing efficiency as the decision-making criterion. The game benefit function of the player is expressed as

$$ue_i^k(\alpha_i) = E_i(k) \tag{24}$$

Comprehensive-type Rational Person: The driver who considers safety and efficiency factors to make comprehensive decisions when interacting, and his(her) benefit function is derived by

$$ub_i^k(\alpha_i) = m_i^k E_i(k) + n_i^k(1 - R_i(k)) \tag{25}$$

where $R_i(k)$ is the comprehensive risk of driver i perceived at k^{th} interval, as formulated in the Eq. 19, E_i^k is the efficient benefit of driver i, which is defined as the speed of the vehicle per the unit time, α_i^k is the specific action performed by driver i, m_i^k and m_i^k respectively represent the driver's weight coefficient for efficiency and safety risk perception, $m_i^k \geq 0$, $n_i^k \geq 0$, $m_i^k + n_i^k = 1$. It should be noted that safety-priority and efficiency-priority drivers are only ideal boundaries and do not exist in reality.

Game theory has traditionally been divided into two categories, the non-cooperative game, and cooperative game(Barron (2013)). In the non-cooperative game, all players make decisions independently and only consider the maximization of their own profit. In the cooperative game, higher overall income can be obtained by reaching a consensus among individuals and forming a coalition(Yang, Huang, Wang, Pei and Yao (2018)). The non-cooperative game and cooperative game represent two kinds of interactive thinking.

In reality, drivers actually have different degrees of cooperative and competitive tendencies, which can be quantified through the index of Social Value Orientation (Wang et al. (2022a)). In our paper, two boundary cases are defined: one is the completely selfish rational person, who will only consider his own targets and maximize his utility when passing the intersection, which leads to a non-cooperative interaction game, the other is the total-altruism rational person, who will completely prioritize the efficiency of others. When two completely altruistic persons appear, both parties will take action with the goal of maximizing the system's total efficiency, which generates a cooperative interaction game. Therefore, to evaluate the competitiveness and cooperation of driver interaction, two types of game models are set, i.e., non-cooperative game and cooperative game.

4.2.1. Non-cooperative Game

In the non-cooperative game, players will determine their strategies independently and aim to maximize their payoff, which leads to competition and can be characterized as a Nash game.

For player i , whose rational style is denoted as $\mu(\mu \in \mu s, \mu e, \mu b)$, the utility at every time interval is u_{t_i}. $\mu s, \mu e, \mu b$ are defined in formula 23,24,25 respectively. Therefore, at k^{th} interval, the optimization objective function of the player i can be characterized as

$$\mathbf{a}_i^{k*} = \arg\max\ u_{t_i}^*(k) = \arg\max \Phi(\mathcal{A}_i^{k-1}, a_k^i) \tag{26}$$

s.t.

$$\|t_i - t_{i^-}\| \geq t_{avoid}, \forall i \in \{C_L, C_S\}, i^- \in \{C_L, C_S\} \backslash \{i\} \tag{27}$$

$$0 \leq v_i(k) \leq v_{max}, \forall i \in \{C_L, C_S\} \tag{28}$$

$$\|a_i(k)\| \leq a_{max}, \forall i \in \{C_L, C_S\} \tag{29}$$

where t_{avoid} is the minimum time to avoid the collision, which is related to the intersection size and speed of the players, v_{max} and a_{max} are the maximum permitted speed under traffic rules and maximum comfortable acceleration driver can choose.

The Lemke-Howson Algorithm (L-HA) is used to solve the Nash equilibrium of the non-cooperative model(Shapley (1974)), which is defined as the competitive result of players.

4.2.2. Cooperative Game

When two completely altruistic players interact, two parties will take action to improve the system's efficiency, which leads to a cooperation game. Different from the non-cooperative game, in the cooperative game framework, drivers will reach cooperative consensus and form coalitions to gain higher overall benefits.

For a cooperative coalition, there exists a set N (containing n players) and eigenfunction $\mathcal{V}$ that maps a subset of players to the real numbers, $\mathcal{V} : 2^n \rightarrow R$. $\mathcal{V}(S)$ represents the total payoff obtained by all members of coalition S through cooperation. In a given coalition game $(\mathcal{V}, N)$, the benefit of any player i in the set at time step k is calculated by Shapely theory as follows:

$$u_i^k = \sum_{S \subseteq N} \sum_{\forall i \in N} \frac{(|S|-1)!(n-|S|)!}{n!} [\mathcal{V}^k(S) - \mathcal{V}^k(S - \{i\})] \tag{30}$$

where $|S|$ denotes the number of members in the coalition S. According to the definition of eigenfunction $\mathcal{V}$ and game profit, it yields that

$$\begin{cases} \mathcal{V}^k[\emptyset] = 0 \\ \mathcal{V}^k[\{a,b\}] = \left(m_a^k E_a(k) + n_a^k(1 - R_a(k)) + (m_b^k E_b(k) \right. \\ \left. + n_b^k(1 - R_b(k)\right) \\ \vdots \\ \mathcal{V}^k[N] = \left(m_1^k E_1(k) + n_1^k(1 - R_1(k)) + (m_2^k E_2(k) \right. \\ \left. + n_2^k(1 - R_2(k)) + \cdots + (m_N^k E_N(k) + n_N^k(1 - R_N(k)\right) \end{cases} \tag{31}$$

$$\mathcal{V}^k(N) = \sum_{\forall i \in N} u_i^k \tag{32}$$

The reason that Eq. 31 always holds is presented as follows.

$$\begin{aligned}\sum_{i\in N} u_i^k &= \frac{1}{|N|!}\sum_{S\subseteq N}\sum_{\forall i\in N}\left(\mathcal{V}^k(S)-\mathcal{V}^k(S-i)\right)\\ &= \frac{1}{|N|!}\sum_{S\subseteq N}\mathcal{V}(N) = \frac{1}{|N|!}|N!|\mathcal{V}(N) = \mathcal{V}(N)\end{aligned} \tag{33}$$

In the cooperative game, solving the optimal action sequence at each time step is equivalent to an optimization problem, and its optimization objective is defined by

$$(a_1^{k*}, a_2^{k*}, \cdots, a_n^{k*}) = \arg\max \sum_{i=1}^{n} \Phi_i^k(\mathcal{A}_i^{k-1}, a_i^k) \tag{34}$$

s.t.

$$\|t_i - t_{i^-}\| \geq t_{avoid}, \forall i \in \{C_L, C_S\}, i^- \in \{C_L, C_S\}\backslash\{i\} \tag{35}$$

$$0 \leq v_i(k) \leq v_{max}, \forall i \in \{C_L, C_S\} \tag{36}$$

$$\|a_i(k)\| \leq a_{max}, \forall i \in \{C_L, C_S\} \tag{37}$$

$$\mathcal{V}(S) + \mathcal{V}(T) \leq \mathcal{S} + \mathcal{T}, \forall S, T \in N, S \cap T = \emptyset \tag{38}$$

The Genetic Algorithm (GA) is used to solve the Pareto optimal issue, which is defined as the cooperative result of the interacting objects(Yang et al. (2018)). The payoff u_i^k of each player in the coalition can be described as follows.

$$\Omega^k = [\Phi_1^k, \Phi_2^k, \cdots, \Phi_n^k] \tag{39}$$

Finally, the optimal action solution results of all players are obtained.

$$\begin{aligned}\mathcal{A}^{k*} &= [\mathcal{A}_1^k, \mathcal{A}_2^k, \cdots, \mathcal{A}_n^k]\\ &= [\mathcal{A}_1^{k-1} \cap a_1^{k*}, \mathcal{A}_2^{k-1} \cap a_2^{k*}, \cdots, \mathcal{A}_1^{k-1} \cap a_1^{k*}]\end{aligned} \tag{40}$$

According to the game strategies executed by two players at k^{th} interval, the motion states of players at $k+1^{th}$ are calculated. Then the game strategy is selected again at $k+1^{th}$ step. The whole modeling and solving process is shown in Algorithm 1.

4.3. Interactive Ability Scoring

The set of rational person actions is then employed as the evaluation criterion of interaction ability, and the interaction performance of the driver is assessed by measuring the gap between actual driver actions and the rational person acceleration sequences. At present, the evaluation of driver decision-making actions is mostly based on trajectory information, such as KL divergence, MSE, mADE (Demetriou, Allsvåg, Rahrovani and Chehreghani (2020)), etc.

However, using trajectory for direct interaction evaluation is not comprehensive, and there are two main problems. On the one hand, because of no time dimension information, the spatial similarity evaluation using the trajectory information can't directly reflect the driver's reaction speed, intensity, and preference when taking action. On the other hand, the excellent interaction trajectories are not unique, and there may be multiple optimal trajectories (represented as multiple equilibrium solutions in the game model).

In contrast, acceleration information can reflect more features. For example, experienced drivers will be smoother in acceleration and deceleration during the interaction, predict the situation in advance and brake in advance, etc., all

Algorithm 1: Game-based Interaction Process.

Input: Initial states $X_i(k)$ of player i ($i \in C$)
Output: The action sequence sets $\mathcal{A}^*$

Initialize time interval $k \leftarrow 0$;
Calculate the conflict point of two players CP_{target};
Choose the player style $\mu(\mu \in \{\mu s, \mu e, \mu b\})$and game type $\tau(\tau \in \{NC, C\})$;
while $k \geq 0$ **do**
  for $i \in C$ **do**
    if *player i have passed the point* CP_{target} **then**
      Break
    end
    Update the total benefit $u_i(k)$ of player i:
    $u_i(k) \leftarrow R_i(k) + E_i(k)$;
    Solve for equilibrium and get strategy $\alpha_i(k)$:
    if $\tau = NC$ **then**
      $\alpha_i(k) \leftarrow$ Solved by L-HA;
    else
      $\alpha_i(k) \leftarrow$ Solved by GA ;
    end
    Update the state of the player:
    $v_i(k) = v_i(k-1) + \alpha_i(k)\Delta t$;
    $s_i(k) = s_i(k-1) + v_i(k)\Delta t$;
    Update $\mathcal{A}_i^k \leftarrow \mathcal{A}_i^{k-1} \cap \alpha_i(k)$;
    $k \leftarrow k + 1$;
  end
  $\mathcal{A}^* \leftarrow \mathcal{A}_i^k$;
end

of which can be extracted from the acceleration sequence. The acceleration sequences here are applied for evaluation, which are regarded as N-dimensional time sequence vectors.

For a specific driving scene, the actual acceleration sequence of interactive object i is expressed as

$$\mathcal{A}_{re}^* = [a_1, a_2, a_3, ..., a_n] \tag{41}$$

The excellent acceleration sequence for the rational person is described as

$$\mathcal{A}_{so}^* = [\hat{a_1}, \hat{a_2}, \hat{a_3}, ..., \hat{a_n}] \tag{42}$$

Therefore, the ability evaluation problem is transformed into the vector similarity evaluation problem. The commonly used similarity evaluation indexes include Manhattan distance and Euclidean distance (Magdy, Sakr, Mostafa and El-Bahnasy (2015)), but these methods ignore many important features of vectors. Based on the morphological similarity distance method, an improved evaluation method is proposed, which takes into account three aspects: Euclidean distance to measure the vector distance, cosine similarity to evaluate the vector direction, and morphological similarity evaluation of time series data, which is more comprehensive than a single index.

The improved morphological similarity distance between vectors $\mathcal{A}_{re}^{n*}$ and $\mathcal{A}_{so}^{n*}$ can be defined as follows.

$$D_{MSD,i}(\mathcal{A}_{re}^*, \mathcal{A}_{so}^*) = D_{ED,i}(\mathcal{A}_{re}^*, \mathcal{A}_{so}^*) * \left(2 - \frac{ASD_i}{SAD_i}\right) \tag{43}$$

$$ASD_i = |\sum_{i=1}^{n} (a_k - \hat{a}_k)| \tag{44}$$

$$SAD_i = \sum_{i=1}^{n} |a_i - \hat{a}_i| \tag{45}$$

where $D_{ED,i}$ denotes the Euclidean distance between $\mathcal{A}^*_{re}$ and $\mathcal{A}^*_{so}$, SAD (Sum of Absolute Differences) is the Manhattan distance between $\mathcal{A}^*_{re}$ and $\mathcal{A}^*_{so}$, ASD (Absolute Sum of Differences) is the absolute value of the sum of dimensional differences between $\mathcal{A}^*_{re}$ and $\mathcal{A}^*_{so}$.

The cosine similarity between $\mathcal{A}^*_{re}$ and $\mathcal{A}^*_{so}$ is defined as follows.

$$Co_i = \frac{\mathcal{A}^*_{so}\mathcal{A}^*_{re}}{\|\mathcal{A}^*_{re}\|\|\mathcal{A}^*_{so}\|} = \frac{\sum_{i=1}^{n} a_1\hat{a_1}}{\sqrt{\sum_{i=1}^{n} a_i^2} + \sqrt{\sum_{i=1}^{n} \hat{a_i}^2}} \tag{46}$$

And then the interactive ability score is defined by

$$S_i = P_{MASD,i} = \frac{Co_i}{1 + D_{MSD,i}} \tag{47}$$

where $S_i \in [-1, 1]$.

Further, the interaction ability score results are divided into five levels, in which level I represents the best interaction ability, and level V represents the worst interaction performance. In the specific evaluation, the one-way ability or the comprehensive ability of interactive vehicles can be scored and rated, and a horizontal comparison will be made.

5. Experiments and Results

In this section, the process of parameter calibration for the model is first described. Then the differences in driver ability in two datasets from three aspects are analyzed, and several cases are selected and mined to observe the drivers' reaction during the interaction. Finally, we discuss the differences between our model and another baseline method, and the comparison results reflect the advantages of our model.

5.1. Data and Scenario

Two datasets are processed for trial evaluation and comparative analysis, as shown in Figure 3. One is the Xianxia-Jianhe Dataset, which is collected from the Xianxia-Jianhe intersection, in Shanghai, China(Ma, Sun and Wang (2017)). Xianxia-Jianhe intersection is a typical two-phase intersection, where left-turn vehicles often interact with straight vehicles and non-motor vehicles. After screening and preprocessing, 54 left-straight interaction events in the dataset are extracted.

The other one is Waymo Left-Turn Motion Dataset, which is filtered and processed from Waymo Open Motion Dataset. Waymo Open Motion Datset is an interaction motion dataset released by Waymo in March 2021, which contains a large number of interactive behaviors in different scenarios such as car following, lane changing, intersection turning, and so on from the United States(Ettinger, Cheng, Caine, Liu, Zhao, Pradhan, Chai, Sapp, Qi, Zhou et al. (2021)). By the steps of lane topological relationship extraction, intersection identification, interaction feature analysis, and behavior recognition of unprotected left turn, 192 groups of unprotected left turn scenarios were screened from this dataset.

In the experiment part, the model parameters are first calibrated with real-world datasets. The differences in drivers' safety, efficiency, and interactive sociality during interaction from the two datasets are evaluated. Besides, a group of control experiments is set up. The risk field model of game safety profit is replaced by a simple prediction index based on PET to observe the impact of the risk field model on the evaluation effect.

5.2. Parameters Calibration for Game Model

The model's accuracy and the evaluation's reliability depend on the calibration of the model parameters. The process and results of the calibration of the parameters are illustrated in detail in this subsection.

The problem of parameter calibration can be regarded as an optimization problem. The optimization objective of the problem is to search for the best set of parameters, which minimizes the gap between drivers' actions and game model solutions. Formally, the optimal objective can be expressed as:

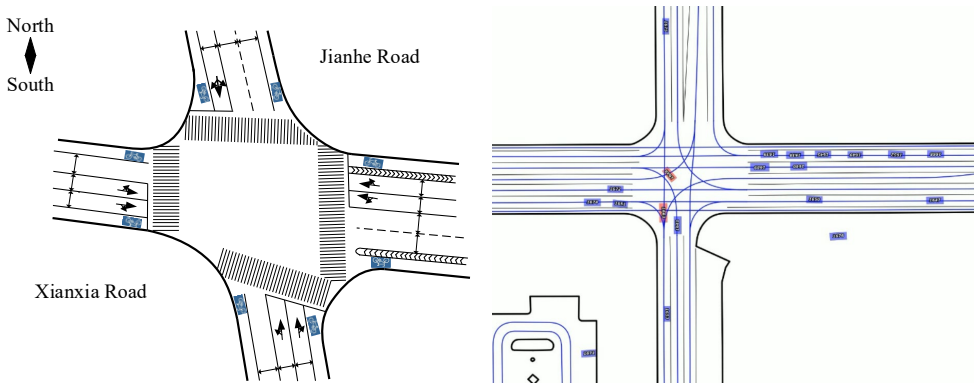

Figure 3: The left turn events from two datasets: (a) the Xianxia-Jianhe Intersection; (b) the intersection from Waymo Left-Turn Motion Dataset.

$$F = \frac{1}{2} \sum_{i \in \{C_L, C_S\}} \frac{1}{N_i} \sum_{j=1}^{N_i} \sum_{t=1}^{T} (a_{ij}^t - \hat{a}_{ij}^t)^2 \tag{48}$$

where a_{ij}^t and $\hat{a}_{ij}^t$ denote the acceleration of the real-world driver and the game model at the t^{th} timestamps, N_i denotes the number of the type i drivers used to be calibrated.

The parameters to be optimized are selected from the part of the risk field model, whose outputs are most affected by the initial parameter settings. They are (1) weighting factors of instantaneous state risk and future state risk w_n; (2) the attenuation coefficients of the attenuation function for speed on the x-axis and y-axis α_x and α_y; (3) the attenuation coefficients of the attenuation function for distance on the x-axis and y-axis β_x and β_y. And the search interval for all parameters is 0.05.

The genetic algorithm (GA) is used to solve the optimization problem. Since the optimization goal of the genetic algorithm is to maximize the fitness function, in order to meet this goal, the fitness function set in the algorithm is:

$$F' = \frac{1}{F} \tag{49}$$

Different population sizes $P(P \in \{10, 20\})$ of the GA and different numbers $N(N \in \{1, 5, 10, 30\})$ of the drivers used to calibrate are set to observe the performance of the algorithm. And other hyperparameters of the GA are shown in Table 1.

The fitness of the objective function with different experimental conditions during the search process is exhibited in Figure 4. The search for all conditions eventually converges within 50 iterations. Moreover, the number of drivers and the population size for GA affect the solving results significantly. Too few or too many drivers make calibration more difficult. Compared with the numbers 1,10, and 30, it is appropriate to calibrate with consider the performance of five drivers. And larger population size produces better calibration performance, contrast population sizes 10 and 20.

And the final calibration results are:

$$[w_n, \alpha_x, \alpha_y, \beta_x, \beta_y] = [0.3157, 0.1053, 0.4737, 0.8421, 0.8947]$$

5.3. Results and Analysis

In this subsection, based on calibrated parameters, the differences of drivers' interactive ability in two datasets are compared. Three kinds of characteristics are evaluated and analyzed, including safety, efficiency, and interactive sociality. The driver's ability scores from all interaction scenarios are calculated and the statistical description for all drivers is obtained, which reveals the difference in driving abilities and styles from different countries and cultures. The average scores of drivers' ability are calculated and the distribution of scores is analyzed. And then, some typical cases are chosen to analyze the results from the non-cooperative game solver and cooperative game solver.

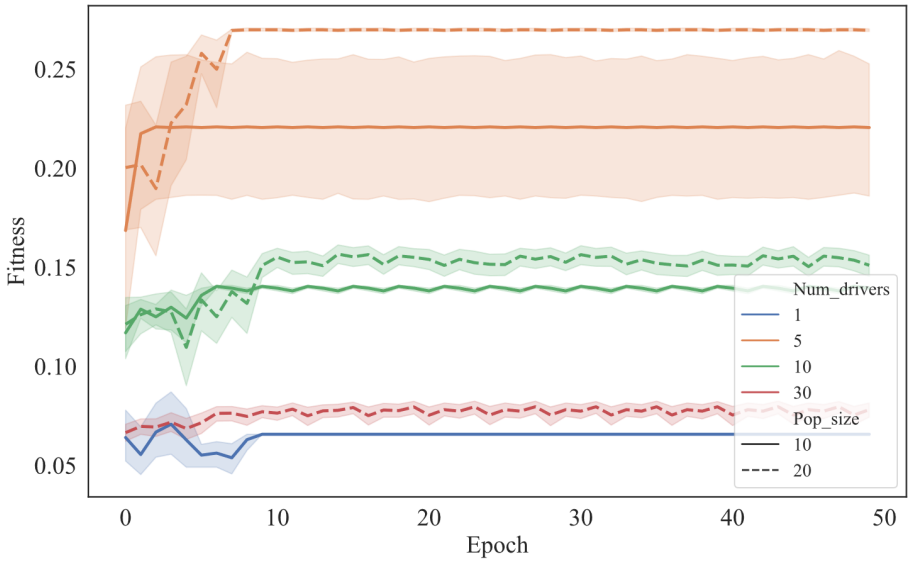

Figure 4: The fitness of the objective function with different hyperparameters during the optimization process.

Table 1
The hyperparameters of the genetic algorithm.

Hyperparameter	Value
DNA Size	10
Crossover Rate	0.6
Mutation Rate	0.01
N Generations	50

5.3.1. Safety and Efficiency Ability

In the non-cooperative game framework, the drivers' performance in three criteria, including safety, efficiency, and comprehensive ability of safety and efficiency, are evaluated. The average scores of left-turn drivers in two datasets is shown in Figure 5.

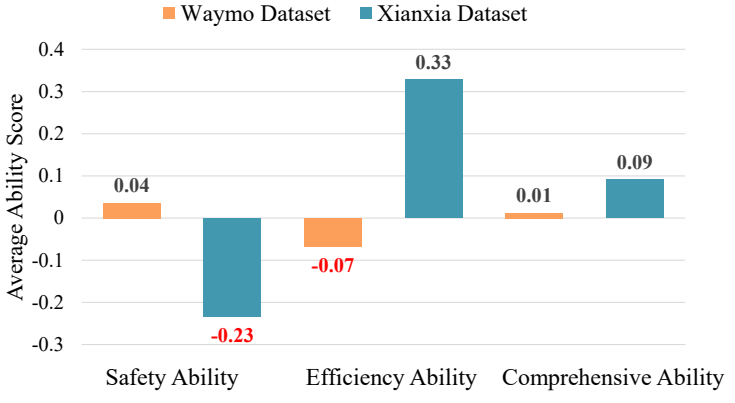

Figure 5: Drivers' average ability score from two datasets.

For comprehensive ability, the average score of drivers in the Waymo Dataset is 0.01, and the average score of drivers in the Xianxia-Jianhe Dataset is 0.09, which indicates that drivers in the Xianxia-Jianhe dataset (hereafter referred to as Xianxia drivers) have better left-turn comprehensive ability than drivers in Waymo dataset (hereafter referred to as Waymo drivers). In terms of safety performance, Waymo drivers score an average of 0.04, while Xianxia drivers score an average of -0.23, indicating that Waymo drivers performed significantly better than Xianxia drivers in safety. For the efficiency performance, Waymo drivers get an average score of -0.07 and Xianxia drivers score an average of -0.33, suggesting Xianxia drivers are more efficient.

The difference in the score distribution between two types of drivers under three criteria is shown in Figure 6, and the distribution of ability grades is shown in Figure 8. In summary, the results show that there is a significant difference in driving preference between Xianxia drivers and Waymo drivers when they make unprotected left turns. Xianxia drivers (from China) pay less attention to safety in order to achieve higher traffic efficiency, while Waymo drivers (from the United States) is more conservative and cared about safety.

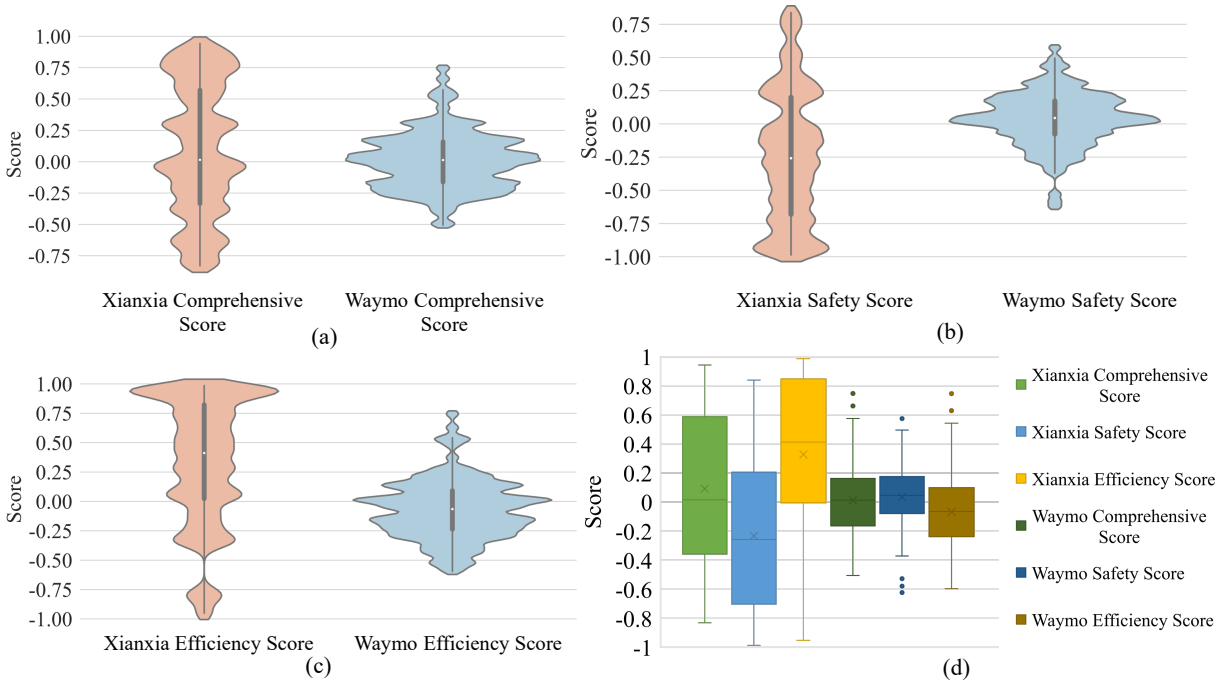

Figure 6: Distribution of driver ability scores: (a) Driver comprehensive ability score violin chart; (b) Driver safety score violin chart; (c) Driver efficiency score violin chart; (d) Box plots of mean scores for the two datasets.

5.3.2. Interactive Sociality

As mentioned above, the levels of competition and cooperation are used to depict interactive sociality. Non-cooperative game and cooperative game frameworks are designed to evaluate the performance of the drivers on the cooperative and competitive. The Nash equilibrium of the non-cooperative game and the Pareto optimal solution of the cooperative game are considered as the ability measuring standard. The results of the drivers' comprehensive ability are shown in Figure 7.

For the same scenario, when drivers' scores in the cooperative game framework exceed the score in the non-cooperative game framework by more than 5%, it is considered that the driver shows more cooperation in the interaction process. When scores of the non-cooperative game exceed the scores of the cooperative game by more than 5%, the drivers are regarded to be more competitive. Otherwise, it is considered that the drivers have both competition and cooperation in the process.

As shown in Table 2, 31.48% of Xianxia drivers show stronger competitiveness, while only 17.58% of Waymo drivers do. 25.93% of Xianxia drivers and 26.37% of Waymo drivers get stronger cooperation. 56.04% of Waymo

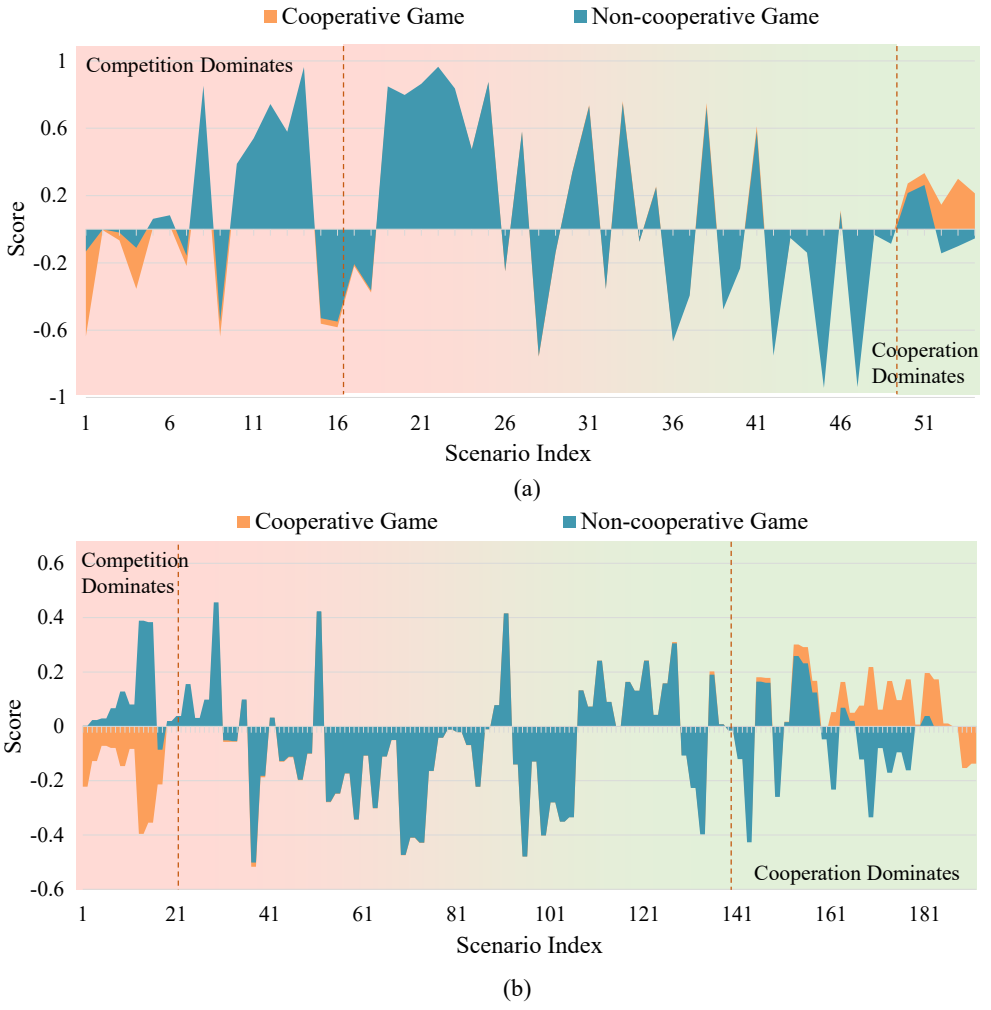

Figure 7: The competition and cooperation ability of drivers from two datasets: (a) The drivers from Xianxia Dataset; (b) The drivers from Waymo Dataset.

Table 2
The percentages of competition and cooperation tendency fro two datasets

Type	Waymo Drivers	Xianxia Drivers
Stronger Competition	17.58 %	31.48 %
The Balance	56.04 %	42.59%
Stronger Cooperation	26.37 %	25.93%

drivers interact with both competition and cooperation, while that percentage of Xianxia drivers is 42.59%. In conclusion, more Xianxia drivers express competitive tendencies, while Waymo drivers are more cooperative tendencies.

5.3.3. Case Analysis

Three cases from different drivers are chosen to analyze the processes of action-taking and interaction with the non-cooperative and cooperative game models.

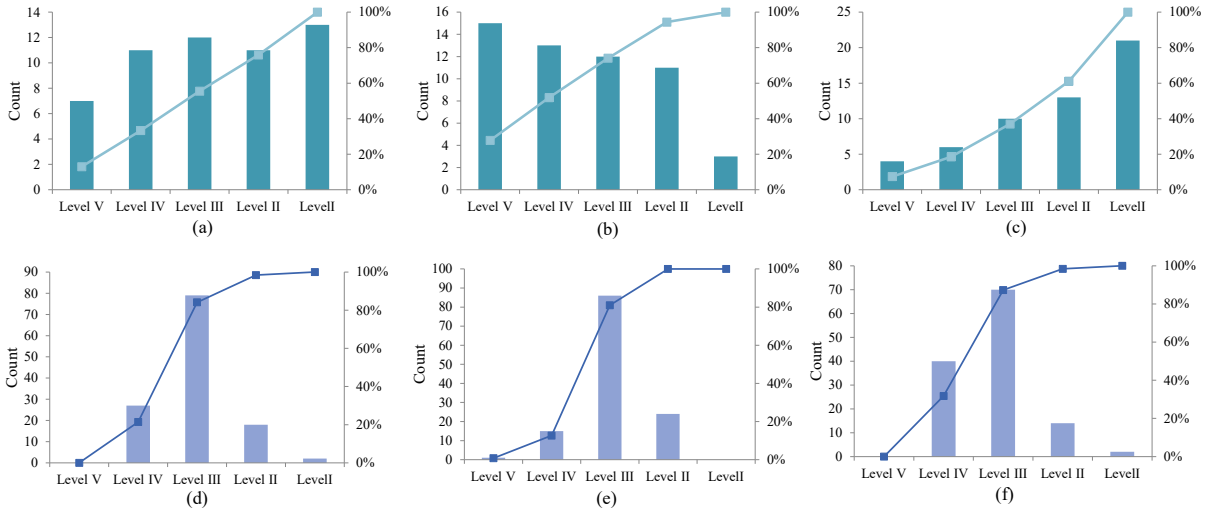

Figure 8: Driving ability class frequency map: (a) Xianxia dataset - Comprehensive capability; (b) Xianxia Dataset - Safety capability; (c) Xianxia dataset - Efficiency capability; (d) Waymo dataset - Comprehensive capabilities; (e) Waymo dataset - Safety capabilities; (f) Waymo dataset - Efficiency capability.

The acceleration information of the three cases is exhibited in Figure 9. In each case, the real-world driver, the non-cooperative game results (in the half left of the subplot), and the cooperative game results (in the half right of the subplot) are discussed.

In case 1, as shown in Figure 9 (a) and (b), the straight real-world driver passed the intersection almost without deceleration, and the left-turning real-world driver decelerated and stopped to give way. However, both the left-turning actions and straight actions solved by the non-cooperative model decelerated and waited for the other driver to pass first, which leads to a dilemma. This may be caused by that both drivers in the non-cooperative game overestimated the safety risk of rushing and chose conservative parking behavior. Different from the waiting dilemma of the non-cooperative game, the left-turning driver in the cooperative game agreed with the straight player and began to accelerate at 20^{th} timestamps, after tentative actions in 2 seconds, which made the solutions from the cooperative game get higher global profit.

Similar features occurred in the second case, as demonstrated in Figure 9 (c) and (d). The two drivers in the non-cooperative game kept on decelerating just like in case 1. Both the straight driver and left-turning driver decelerated first and then accelerated, despite the action of the straight driver being more of a priority. Meanwhile, the left-turning driver in the cooperative game oscillated between acceleration and deceleration and finally sped through the intersection. More frequent action adjustments led to higher payoffs for two players, but it also resulted in a decline in comfort, because comfort was not taken into account in the game model this paper proposed.

A more obvious and vivid negotiation and the game process can be seen in the third case, exhibited in Figure 9 (e) and (f). Both real-world drivers did not significantly adjust their maneuvers, while drivers in the game model interacted more frequently. When approaching the intersection, two drivers in the non-cooperative model switched from acceleration to deceleration after 2 seconds, and then the left-turning driver kept on accelerating. The actions of the two drivers in the cooperative game were more dynamic. After the left-turning driver decelerated, the straight driver tried to accelerate to tune his motion states. When the situation was clear, the left-turning driver began to accelerate, and the straight driver slowed down accordingly.

Overall, compared with real-world drivers, the drivers in the game model could react and modify their actions more quickly. More global benefits could be obtained by the drivers in the cooperative game model, which well explains the advantages and characteristics of the cooperative game. It also can be seen (Figure 9 (a), (c)) that the two drivers both showing stronger competition would not gain a better interaction, even though both of those are definitely rational.

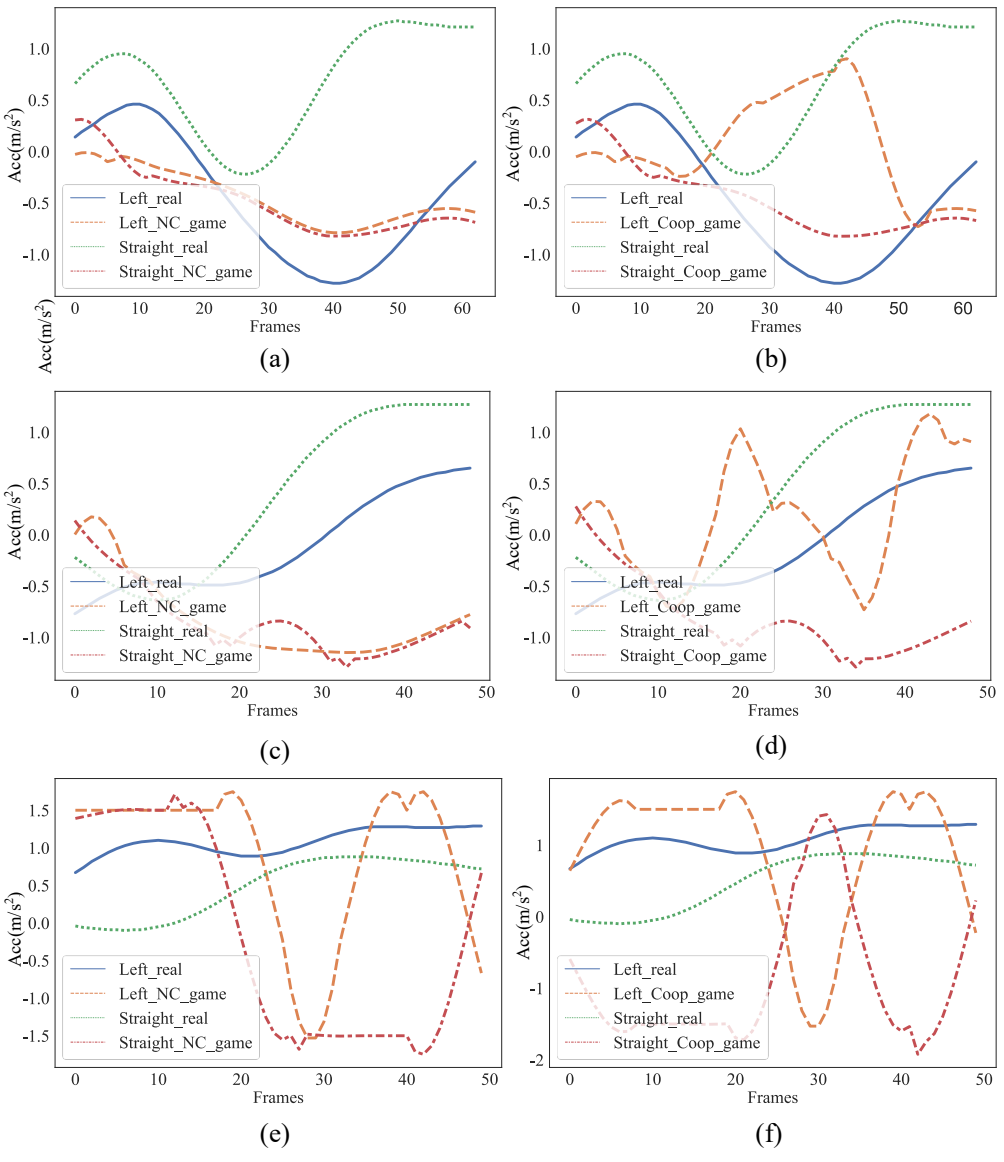

Figure 9: The results of acceleration from three cases with the non-cooperative game and cooperative game, (a),(b): Scenario 18; (c),(d) : Scenario 33; (e), (f) : Scenario 40.

5.4. Comparison with the baseline method

In order to show the reliability of our model, we compare the model with a baseline evaluation index PET. Since PET can only evaluate the safety of the interaction results, in order to ensure the rationality of the comparative analysis, we replace the risk model in the evaluation framework with the PET indicator to obtain a baseline model. The results of the two models are analyzed.

When using the PET metric, player i 's payoff function is:

$$ub_i^k(\alpha_i) = m_i^k E_i(k) + n_i^k \left(PET_i(k)\right) \tag{50}$$

$$PET_i(k) = |\left(\frac{dis_i(k)}{v_i(k+1)+\epsilon} - \frac{dis_o(k)}{v_o(k+1)+\epsilon}\right)| \tag{51}$$

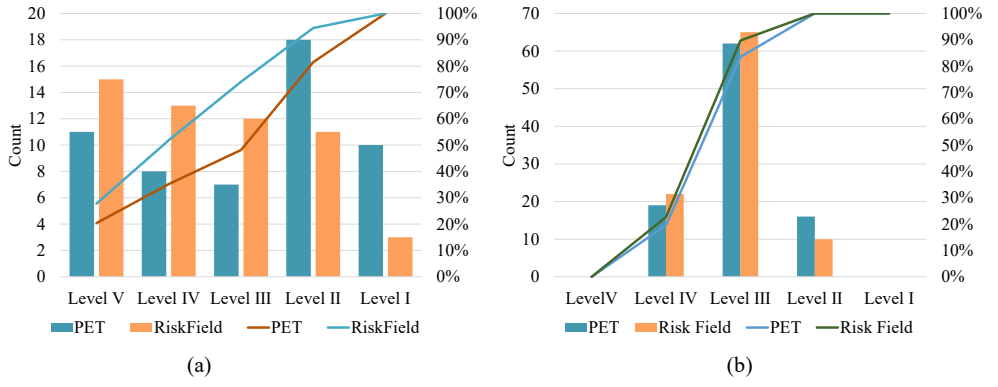

Figure 10: Comparison of the distribution of driving ability grades.(a) Xianxia-Jianhe Dataset; (b) Waymo Dataset.

where driver o is the target of interaction for driver i, $dis(k)$ represents the distance between player i and conflict point at k^{th} interval, $v(k+1)$ represents player's velocity at $k+1^{th}$ interval, ϵ is a minimum to ensure existence of the function.

The drivers' performance with two different safety payoff functions is shown in Figure 10. Compared with the PET index, the scores of safety ability calculated based on the risk field index are lower, which indicates that the risk field index is more cautious and conservative than the PET index. In the Xianxia-Jianhe Dataset, the difference between scores of the two standards is obvious, while in the Waymo Dataset, the difference is insignificant, which may be related to the conservative behaviors of Waymo drivers.

Meanwhile, the PET of all interaction events in two datasets is calculated and counted. Generally, the smaller PET of interaction events are, the more aggressive interaction and the higher security risks occur. PET distribution and average results are shown in Figure 11. The average PET of interaction events in the Xianxia Dataset is smaller than Waymo Dataset, and the difference in data distribution between the two has been verified by t-test for significance, as shown in Table 3 and Table 4, which indicates that PET analysis alone can also find: Xianxia drivers are higher than Waymo drivers in driving aggression and efficiency, but weaker than Waymo drivers in safety performance, which is consistent with the conclusion obtained by using the interactive evaluation framework.

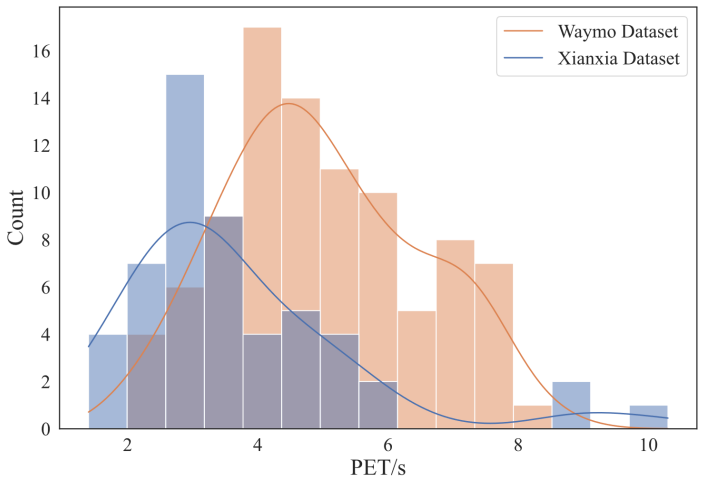

Figure 11: PET frequency distribution of interaction events from the two datasets.

Table 3
Descrition Statistics of PET from two datasets.

Group	Mean/s	Std. Deviation	Std. Error Mean
Xianxia Drivers	3.6906	1.8081	0.2484
Waymo Drivers	4.9913	1.4950	0.1559

Table 4
Independent T-Test results of two datasets.

	Levene's Test for Equality of Variances		T-test for Equality of Means				
	F	Sig.	t	df	Sig. (2-tailed)	Mean Difference	Std. Error Difference
Equal variances assumed	0.127	0.722	-4.668	143	0	-1.30074	0.27865
Equal variances not assumed			-4.436	92.796	0	-1.30074	0.29322

6. Conclusions

In the human-machine mixed driving environment, it is very important for the decision-making of AVs to understand drivers' interaction behaviors and evaluate their interaction abilities. In our work, a three-stage interaction ability evaluation framework is proposed, including Interaction Risk Perception Modeling, Interaction Process Modeling, and Interaction Ability Scoring, which is universal for challenging interaction scenarios and can assess the driver's ability during the interaction process.

The interaction behavior of drivers is modeled based on different types of game models, and the safety profits of the model are qualified by the Risk Perception module. The action output of the game model is taken as the action of a rational person, which is regarded as the ability evaluation standard, and drivers' ability is evaluated by measuring the action difference between drivers and rational persons. At the same time, we propose an improved evaluation index based on morphological similarity distance to score and evaluate drivers' ability in the real world from three dimensions: safety, efficiency, and interactive sociality. As one of the most complex and high-risk scenarios, an unprotected left-turn scene at the intersection is studied as a typical instance. Two datasets are analyzed to compare the left-turn interaction ability of drivers from Shanghai, China, and the United States. The conclusion can be drawn that there are significant differences in different dimensions of driving ability between Chinese and American drivers.

This work presents a basic framework, which can be extended to some common scenarios easily, such as car-following, right turns, and U-turns at intersections. Meanwhile, more evaluation indicators will be considered in the future, including comfort, fairness, and transportation system efficiency. The method of this work can also be applied to the interactive ability evaluation and interactive anthropomorphism analysis of AVs in the future.

7. Acknowledgments

This work was supported in part by the National Natural Science Foundation of China (52232015), in part by the Fundamental Research Funds for the Central Universities (No. 2022-5-ZD-02 and No. 22120220434), and in part by the Zhejiang Laboratory (2021NL0AB02).

References

Barron, E.N., 2013. Game theory: an introduction. volume 2. John Wiley & Sons.

Cai, J., Hang, P., Lv, C., 2021. Game theoretic modeling and decision making for connected vehicle interactions at urban intersections, in: 2021 6th IEEE International Conference on Advanced Robotics and Mechatronics (ICARM), pp. 874–880. doi:10.1109/ICARM52023.2021.9536147.

Crizzle, A.M., Classen, S., Bedard, M., Lanford, D., Winter, S., 2012. Mmse as a predictor of on-road driving performance in community dwelling older drivers. Accid Anal Prev 49, 287–292.

Demetriou, A., Allsvåg, H., Rahrovani, S., Chehreghani, M.H., 2020. Generation of driving scenario trajectories with generative adversarial networks, in: 2020 IEEE 23rd International Conference on Intelligent Transportation Systems (ITSC), IEEE. pp. 1–6.

Doi, A, 1994. Development of a rear-end collision avoidance system with automatic brake control. Jsae Review 15, 335–340.

Ettinger, S., Cheng, S., Caine, B., Liu, C., Zhao, H., Pradhan, S., Chai, Y., Sapp, B., Qi, C.R., Zhou, Y., et al., 2021. Large scale interactive motion forecasting for autonomous driving: The waymo open motion dataset, in: Proceedings of the IEEE/CVF International Conference on Computer Vision, pp. 9710–9719.

Fiorentino, D.D., Parseghian, Z., 1997. Time-to-collision: A sensitive measure of driver interaction with traffic in a simulated driving task, in: Proceedings of the Human Factors and Ergonomics Society Annual Meeting, SAGE Publications Sage CA: Los Angeles, CA. pp. 1028–1031.

Hillenbrand, J., Spieker, A.M., Kroschel, K., 2006. A multilevel collision mitigation approach—its situation assessment, decision making, and performance tradeoffs. IEEE Transactions on Intelligent Transportation Systems 7, 528–540.

Kathib, O., 1986. Real-time obstacle avoidance for manipulators and mobile robots. Springer New York .

Keogh, E., 2002. Exact indexing of dynamic time warping - sciencedirect. VLDB '02: Proceedings of the 28th International Conference on Very Large Databases , 406–417.

Li, D., Liu, G., Xiao, B., 2021. Human-like driving decision at unsignalized intersections based on game theory. arXiv e-prints .

Li, D., Liu, G., Xiao, B., 2022. Human-like driving decision at unsignalized intersections based on game theory. Proceedings of the Institution of Mechanical Engineers, Part D: Journal of Automobile Engineering , 09544070221075423.

Li, L., Gan, J., Ji, X., Qu, X., Ran, B., 2020. Dynamic driving risk potential field model under the connected and automated vehicles environment and its application in car-following modeling. IEEE Transactions on Intelligent Transportation Systems PP, 1–20.

Little, J.J., Gu, Z., 2001. Video retrieval by spatial and temporal structure of trajectories, in: Yeung, M.M., Li, C.S., Lienhart, R.W. (Eds.), Storage and Retrieval for Media Databases 2001, International Society for Optics and Photonics. SPIE. pp. 545 – 552. URL: https://doi.org/10.1117/12.410966, doi:10.1117/12.410966.

Liu, R., He, J., Zhu, X., 2019. Potential risk assessment algorithm in car following, in: WCX SAE World Congress Experience.

Ma, Z., Sun, J., Wang, Y., 2017. A two-dimensional simulation model for modelling turning vehicles at mixed-flow intersections. Transportation Research Part C: Emerging Technologies 75, 103–119.

Magdy, N., Sakr, M.A., Mostafa, T., El-Bahnasy, K., 2015. Review on trajectory similarity measures, in: 2015 IEEE seventh international conference on Intelligent Computing and Information Systems (ICICIS), IEEE. pp. 613–619.

Markkula, G., Madigan, R., Nathanael, D., Portouli, E., Lee, Y.M., Dietrich, A., Billington, J., Schieben, A., Merat, N., 2020. Defining interactions: A conceptual framework for understanding interactive behaviour in human and automated road traffic. Theoretical Issues in Ergonomics Science 21, 728–752.

Miller, R., Huang, Q., 2002. An adaptive peer-to-peer collision warning system, in: IEEE Vehicular Technology Conference.

Nilsson, M., Thill, S., Ziemke, T., 2015. Action and intention recognition in human interaction with autonomous vehicles, in: " Experiencing Autonomous Vehicles: Crossing the Boundaries between a Drive and a Ride" workshop in conjunction with CHI2015.

Norris, F.H., Matthews, B.A., Riad, J.K., 2000. Characterological, situational, and behavioral risk factors for motor vehicle accidents: a prospective examination. Accident Analysis and Prevention 32, 505–515.

Parkin, J., Clark, B., Clayton, W., Ricci, M., Parkhurst, G., 2016. Understanding interactions between autonomous vehicles and other road users: A literature review .

Qi, W., Wang, W., Shen, B., Wu, J., 2020. A modified post encroachment time model of urban road merging area based on lane-change characteristics. IEEE Access 8, 72835–72846.

Rahmati, Y., Hosseini, M.K., Talebpour, A., 2021. Helping automated vehicles with left-turn maneuvers: a game theory-based decision framework for conflicting maneuvers at intersections. IEEE Transactions on Intelligent Transportation Systems .

Schubert, R., Adam, C., Obst, M., Mattern, N., Leonhardt, V., Wanielik, G., 2011. Empirical evaluation of vehicular models for ego motion estimation, in: 2011 IEEE intelligent vehicles symposium (IV), IEEE. pp. 534–539.

Schuhmann, T., Hofmann, W., Werner, R., 2011. Improving operational performance of active magnetic bearings using kalman filter and state feedback control. IEEE Transactions on Industrial Electronics 59, 821–829.

Shalev-Shwartz, S., Shammah, S., Shashua, A., 2017. On a formal model of safe and scalable self-driving cars .

Shalev-Shwartz, S., Shammah, S., Shashua, A., 2018. Vision zero: on a provable method for eliminating roadway accidents without compromising traffic throughput. arXiv preprint arXiv:1901.05022 .

Shapley, L.S., 1974. A note on the lemke-howson algorithm, in: Pivoting and Extension. Springer, pp. 175–189.

Tan, H., Lu, G., Liu, M., 2021. Risk field model of driving and its application in modeling car-following behavior. IEEE Transactions on Intelligent Transportation Systems .

Tetsuya, Nakamura, Keishi, Taki, Hiroki, Nomiya, Kazuhiro, Seki, Kuniaki, Uehara, 2013. A shape-based similarity measure for time series data with ensemble learning. Pattern Analysis Applications .

Tian, R., Li, N., Kolmanovsky, I., Yildiz, Y., Girard, A.R., 2020. Game-theoretic modeling of traffic in unsignalized intersection network for autonomous vehicle control verification and validation. IEEE Transactions on Intelligent Transportation Systems .

Wang, J., Wu, J., Zheng, X., Ni, D., Li, K., 2016. Driving safety field theory modeling and its application in pre-collision warning system. Transportation research part C: emerging technologies 72, 306–324.

Wang, W., Wang, L., Zhang, C., Liu, C., Sun, L., 2022a. Social interactions for autonomous driving: A review and perspective. arXiv preprint arXiv:2208.07541 .

Wang, W., Wang, L., Zhang, C., Liu, C., Sun, L., 2022b. Social interactions for autonomous driving: A review and perspective. URL: https://arxiv.org/abs/2208.07541, doi:10.48550/ARXIV.2208.07541.

Wang, W., Wang, W., Wan, J., Chu, D., Lu, L., 2019. Potential field based path planning with predictive tracking control for autonomous vehicles, in: 2019 5th International Conference on Transportation Information and Safety (ICTIS).

Xiong, X., Wang, M., Cai, Y., Chen, L., Farah, H., Hagenzieker, M., 2019. A forward collision avoidance algorithm based on driver braking behavior. Accident Analysis Prevention 129, 30–43.

Yang, Z., Huang, H., Wang, G., Pei, X., Yao, D.y., 2018. Cooperative driving model for non-signalized intersections with cooperative games. Journal of Central South University 25, 2164–2181.

Zhao, X., Li, Q., Xie, D., Bi, J., Lu, R., Li, C., 2018. Risk perception and the warning strategy based on microscopic driving state. Accident Analysis Prevention 118, 154–165. URL: https://www.sciencedirect.com/science/article/pii/S0001457518300630, doi:https://doi.org/10.1016/j.aap.2018.02.012.